Arabian Journal of Chemistry (2019) **12**, 1607–1614

King Saud University

Arabian Journal of Chemistry

www.ksu.edu.sa
www.sciencedirect.com

ORIGINAL ARTICLE

Mineral characterization of the Oum El Khacheb phosphorites (Gafsa-Metlaoui basin; S Tunisia)

Haykel Galai [a,*], **Faouzi Sliman** [b]

[a] *Institut National de Recherche et d'Analyse Physico-chimiques, 2026 Technopole de Sidi Thabet, Tunisia*
[b] *Centre de Recherche Metlaoui Compagnie des Phosphates de Gafsa, Tunisia*

Received 12 March 2013; accepted 8 October 2014
Available online 24 October 2014

KEYWORDS

Phosphorite;
Mineralogy;
Quantitative XRD;
TGA–DTA

Abstract The mineralogy of the Tunisian phosphatic series of the Jebel Oum El Khacheb deposit which belongs to the Gafsa-Metlaoui basin, located in the South of Tunisia, was studied. Chemical and mineralogical characterization of eight representative samples (2 mm–70 μm) were undertaken by X-ray diffraction, thermal analysis TG/DTA, Carbon and Sulfur analyzer and Atomic Absorption Spectroscopy. It was revealed that each phosphatic layer contains various silicates and carbonates. The X-ray diffraction results were supported by the Rietveld method to confirm the presence of certain minor phases (calcite, dolomite, bassanite and anorthoclase). The precision and accuracy of the quantitative-phase analysis, using the Rietveld method as a routine tool for process control, were highlighted.

1. Introduction

Large quantities of phosphate are used in agricultural and other industries (Notholt et al., 1989; Locardi et al., 1993). In Tunisia, nearly 80% of commercially-produced phosphate is transformed through chemical-processing industries (production of phosphoric acid and fertilizer minerals). It is well known that the gangue minerals are the cause of the problems that arise during ore extraction, phosphate processing or its chemical valorization. They constitute the main wastes deriving from the processing of these ores. The processing techniques of phosphate ores depend on the type of phosphate minerals existing in the ores as well as the associated gangue minerals (Abouzeid, 2008).

The sedimentary phosphorites contain apatite, as a main mineral and a relatively important quantity of associated minerals. These minerals sometimes occur as clear separated layers or mixed with phosphate ore. The structure of apatite, $Ca_{10}(PO_4)_6X_2$ ($X{=}F^-$, OH^-, Cl^-, CO_3^{2-}) is very tolerant to ionic substitutions (Tõnsuaadu et al., 2012). Carbonates and sulfates are able to substitute for part of the phosphate (Veiderma et al., 2005). Likewise, Ca may be replaced in part by U, lanthanide rare earths or certain other trace metals such as Cd, Zn, or non-metals such as Mg, Sr or Ba. The estimation of the unit parameter of the cell-value constitutes a crystallographic expression of the

* Corresponding author. Tel.: +216 71 537 666; fax: +216 71 537 688.
E-mail address: hgalai@yahoo.fr (H. Galai).
Peer review under responsibility of King Saud University.

Production and hosting by Elsevier

http://dx.doi.org/10.1016/j.arabjc.2014.10.007

apatite composition. Abouzeid (2008) and Mostafa et al. (2000) reported that the correlation between physico-chemical characteristics of different apatites and their crystallographic structures could be correlated with their natural chemical reactivity as direct fertilizers. Moreover calcareous minerals reduce the chemical reactivity of phosphate ores while a greater degree of carbonate substitution for phosphate in the apatite structure tends to make the rock more reactive when directly applied to the soil (El-Jalead et al., 1980; Pan and Darvell, 2010).

Tunisian phosphate ore is composed mainly of carbonate-apatite, silica or chert (microcrystalline quartz, macrocrystalline quartz, chalcedony, opal), carbonates (calcite, dolomite), and also gypsum, organic matter, and clay matter (Sassi, 1974; Béji-Sassi, 1985, 1999; Chaabani, 1995; Galfati et al., 2010; Zaier, 1999).

The enrichment of phosphate, in the Gafsa-Metlaoui basin, is based on the elimination of barren components (clays, carbonates, silica, etc.) contained in the crude ore by performing a wet classification. This is conducted in order to eliminate the fraction >2 mm (high cut-off), perform sieving and obtain fine fraction <70 microns (low cut-off) by hydrocycloning. The clayey matrix is removable by simple washing, while a siliceous or carbonated one displays the features of a cement kind which is not easy to eliminate.

Hence the performance of the phosphate deposit and its upgrading are governed not only by elemental composition but also by its mineralogy. Therefore, XRD is considered as a useful technique in the identification and quantification of minerals contained in phosphates. Moreover X-ray powder diffraction, combined with the Rietveld full pattern, is now widely used in mining and cement industry as effective on stream-analysis technique coupled with automation process. However, the quantification of such complex mixtures (Omotoso et al., 2006; León-Reina et al., 2009; Kampata et al., 2000) remains complex for a number of reasons: (i) there are many phases, with strong peak overlap; (ii) some phases crystallize in platy shapes which display preferred orientation effects; (iii) phases can crystallize as several polymorphs (e.g. silica); (iv) the number of irradiated crystallites may not be high enough to ensure a random orientation for all diffraction planes; and (v) the atomic impurities inside each phase are not known (vi), unknown amounts of amorphous phases with unknown compositions and (vii) diffraction limit for minor mineral detection. Other sources of errors are connected to the preparation of powder, on the one hand, and the refinement strategy as the simulation involves a large number of parameters, on the other hand. Also, the accuracy and degree of uncertainty of such analysis are not easy to assess.

The objective of this work is to determine the mineral characterization of the phosphate ore extracted from eight layers of Oum El Khacheb deposit. The combination of several techniques and XRD, such as the thermal analysis TG/DTA, carbon and sulfur analysis, atomic absorption spectroscopy to analyze these samples with slight compositional variation, would be mandatory to identify minor mineral and to constrain the phase concentration.

2. Sampling and experimental

Phosphate samples were collected from the outcrops of the Oum El Khacheb locality (Fig. 1). The phosphate series is divided into nine layers. Eight samples were collected and denoted as PN-1, PN-2, ...PN-8 according to the position of workable phosphate layers from bottom to top. The phosphorite is treated by crushing, washing, and desliming, for the recovery of 70 μm–2 mm fraction. This process is applied in the Tunisian phosphate industry.

The atomic absorption spectroscopy (Analytik jena, NOVAA 400) was used to determine the element of composition (Al, Ca, Fe, K, Mg, Na, P, and Si) of samples. Carbon and sulfur were measured by combustion and infrared detection (HORIBA, EMIA-220V). All chemical analyses were conducted with experimental errors lower than 5%. X-ray diffraction analysis was carried out by a "Philips MPD1880-

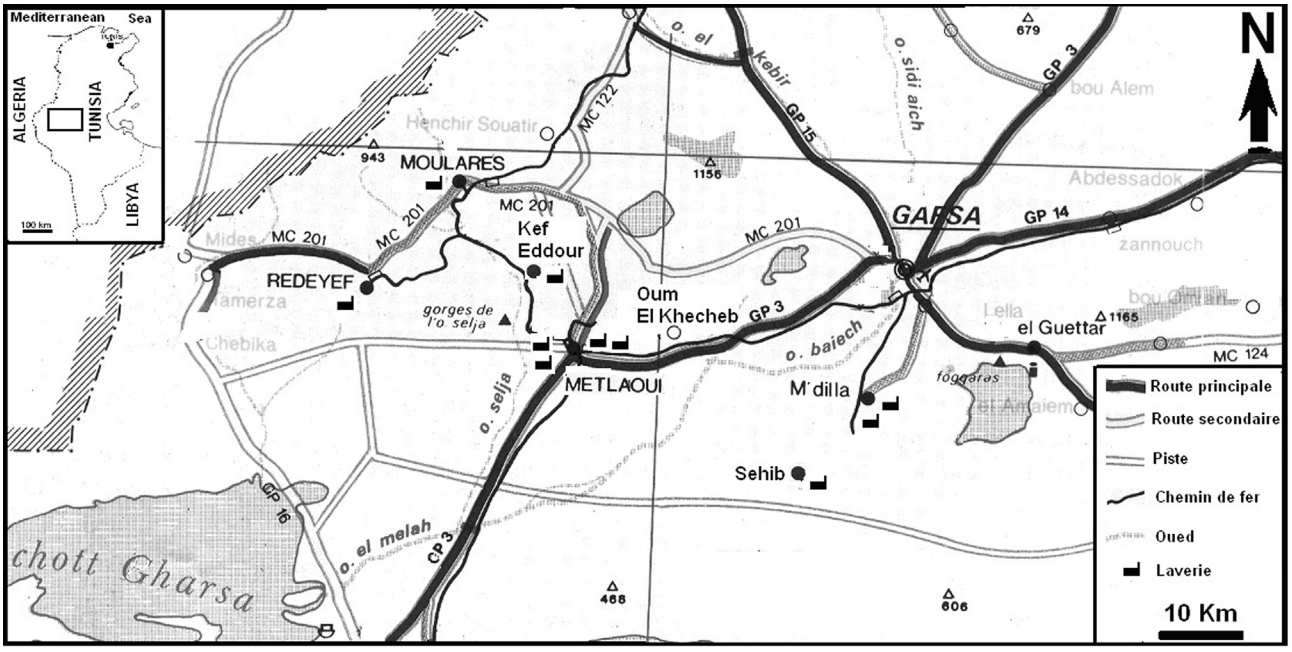

Figure 1 Location of the Oum El Khacheb.

PW1710'' diffractometer using $\lambda_{CuK\alpha}$ radiation, in the 2 °– 80° interval with a step size of 0.02 ° and counting time of 20s/step. The quantification phase was performed on one sample by the Rietveld method (R-QPA), using a PANalytical X'Pert HighScore Plus program. The sample subjected to Rietveld refinement was ground in an agate mortar. Thermal analyses (TG/DTA) were performed in a simultaneous thermoanalysis apparatus ''Setaram Setsys'' with a heating rate of 10 °C/min in helium atmosphere. This analysis was conducted in order to determine mineral transformations during the heating process up to 1450 °C. To characterize the type of apatite, FTIR analysis was performed by BRUKER instrument (VERTEX 70) using an ATR with monoreflexion.

3. Results and Discussion

The chemical analysis conducted on the eight samples, representative of the considered workable layers, shows (Table 1) that the P_2O_5 contents range from 25.88 to 29.5% and reveal that samples contain high amounts of SiO_2 that may reach 8.66%. Small amounts of clay minerals are detected since Al_2O_3 does not exceed 0.4%. Significant amounts of CO_2 and SO_3, are present, ranging from 2.05 to 3.45% and from 6.84 to 9.53%, respectively. Concentrations of magnesium and sodium, which are related generally to dolomite and apatite (Galfati et al., 2010; Bigi et al., 1996) are almost invariable. The amount of organic carbon ranges from 0.35 to 0.83%.

The diffractograms of phosphate ore samples (Fig. 2) show that the main mineral is located close to carbonate apatite (JCPDS n 031-0267), while the quantities and nature of gangue minerals vary from one sample to another.

Different silica minerals are detected. Sample PN-8 contains a high quantity of quartz. Opal-CT and tridymite exist in some samples (PN-4, PN-5 and PN-8). A considerable amount of calcite is observed in the sample PN-1. The samples PN-3 and PN-4 are characterized by the presence of gypsum.

Table 1 Chemicals analysis of the studied eight phosphate samples.

Layer/%	P_2O_5	CaO	SiO_2	MgO	Na_2O	Fe_2O_3	K_2O	Al_2O_3	SO_3 [+]	CO_2 [+]	CO_2 min [‡]	C_{org} [§]
PN1	26.74	43.49	8.66	0.47	1.67	0.18	0.05	0.07	2.05	6.43	5.13	0.35
PN2	29.51	47.25	3.58	0.46	1.67	0.21	0.06	0.11	2.77	8.36	7.05	0.36
PN3	28.54	46.78	5.13	0.47	1.66	0.18	0.06	0.25	2.95	7.66	5.41	0.61
PN4	28.45	46.30	4.60	0.47	1.52	0.26	0.08	0.15	1.85	7.33	5.20	0.58
PN5	27.86	45.34	5.29	0.62	1.62	0.30	0.08	0.41	3.10	7.05	4.94	0.58
PN6	28.91	46.05	2.25	0.5	1.47	0.26	0.07	0.32	2.01	6.84	5.17	0.45
PN7	28.64	45.89	2.78	0.51	1.54	0.21	0.10	0.07	3.32	7.91	6.25	0.45
PN8	25.88	43.56	5.61	0.57	1.56	0.26	0.16	0.15	3.45	9.53	6.5	0.83

[+] Total carbon and sulfur inferred from elementary analysis by combustion and infrared detection.
[‡] CO_2 released in the temperature range 575–900 °C as recorded by TG curves.
[§] Organic carbon deduced from total carbon taking into account mineral carbon.

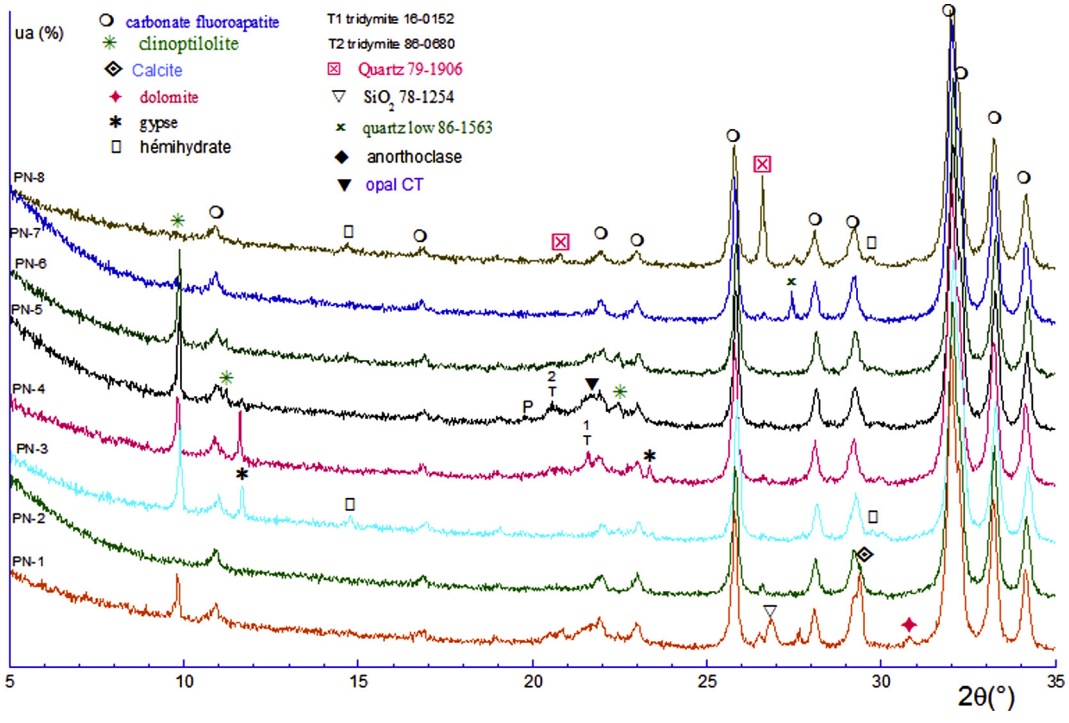

Figure 2 XRD patterns of the studied eight phosphate ore samples.

Clinoptilolite is detected in all samples except for PN-2 and PN-8.

All FTIR spectra (Fig. 3) are reminiscent of a B-type carbonate apatite (Lafon et al., 2003), exhibiting CO_3 bands at 1419 (ν_3) and 870 (ν_2). There is no evidence of the presence of OH^- ion, as the characteristic absorptions around 3600 and 630 cm^{-1} are not observed (Rodriguez-Lorenzo, 2005; Wilson et al., 2004).

Figs. 4 and 5 give the plots of mass loss vs. temperature and the calorimetric plots, respectively.

TG curves show that there are four stages of mass loss profile. The low temperature phase, below 180 °C, corresponds to water removal (1–2%). The second stage of decomposition is related to hydrocarbon materials loss (2–3%) between 180 and 450 °C. Carbonate dissociation (5–7%) occurs within the 650–900 °C temperature range. The final stage is related to sulfate (SO_3) decomposition. This one is released essentially from apatite at 1200 °C (Petkova et al., 2011). Sample PN-8 shows the largest amount of released SO_3 as expected by sulfur analysis (Table 1).

Most DTA curves show a strong exothermic reaction with a peak of 722 °C, which is due to the carbonate-apatite recrystallization. This phenomenon seems to be overlapped by the endothermic effect at 750 °C caused by the dissociation of calcite. For the sample PN-8, the decarbonation of carbonate-apatite is shifted to a relatively higher temperature, which is

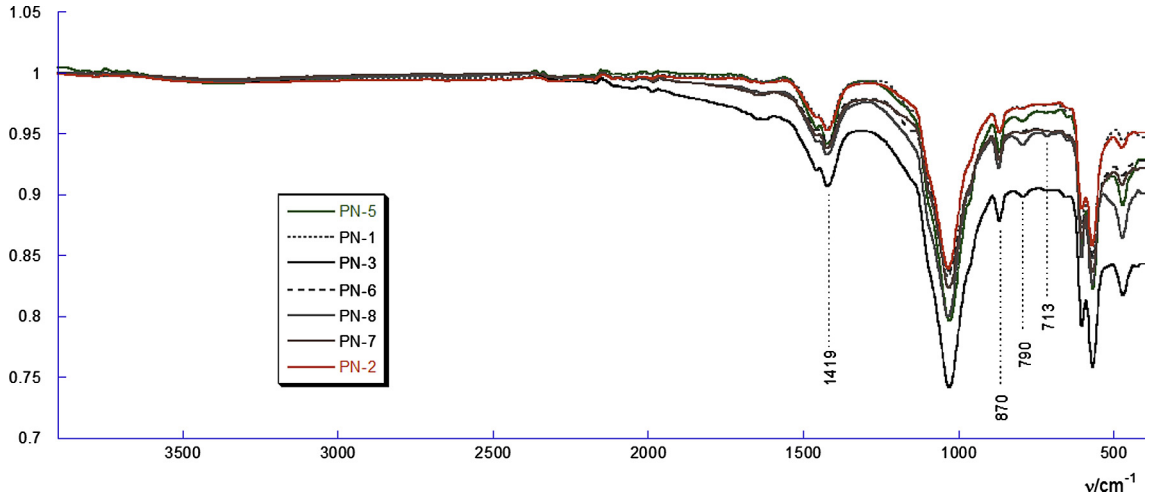

Figure 3 FTIR spectra of the studied eight phosphate samples.

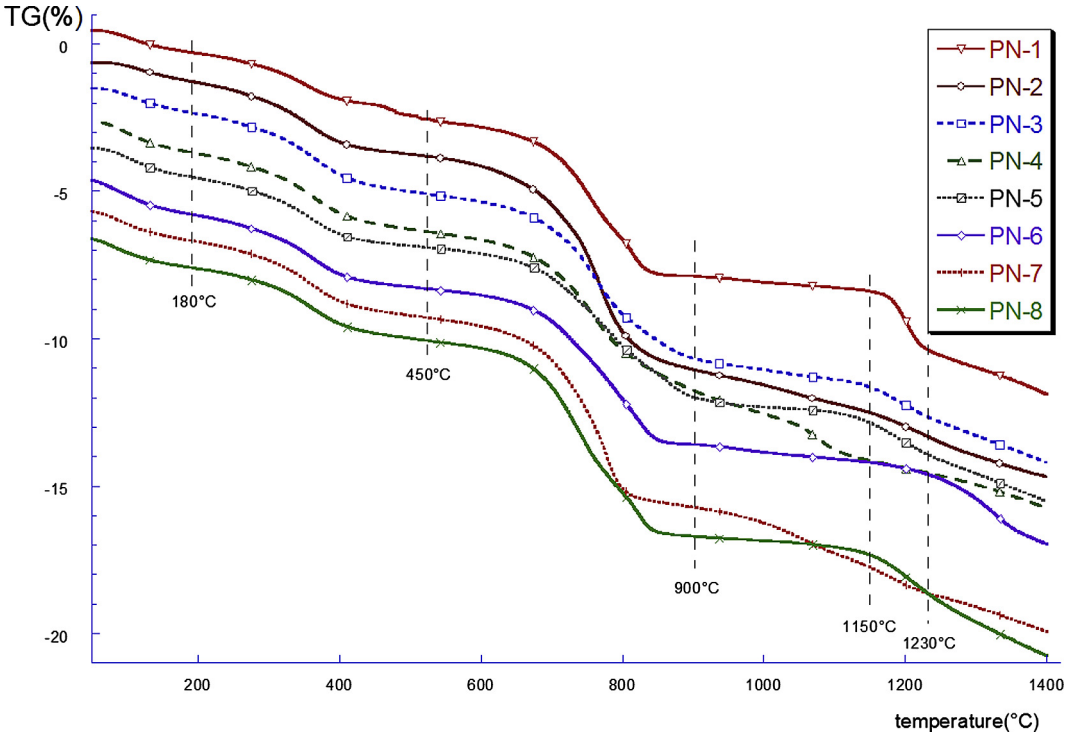

Figure 4 TG curves of the studied eight phosphate ore samples.

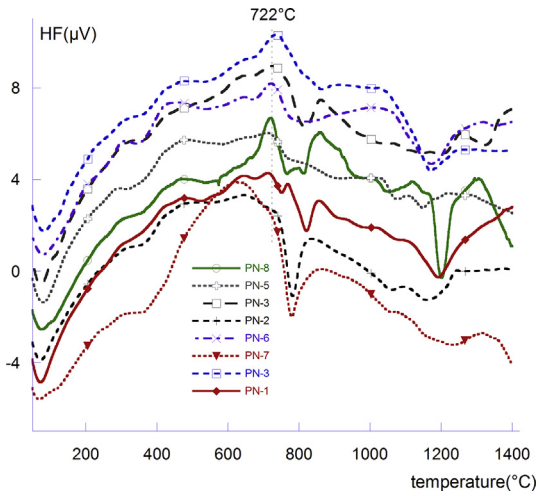

Figure 5 DTA curves of the studied eight phosphate ore samples.

probably due to the release of CO_2 from calcite. Moreover, it is rather difficult to distinguish the decarbonation behavior due to the overlapping of the CO_2 release from both calcite and apatite. In addition, several works (El-Jalead et al., 1980; Lafon et al., 2003; Vilbok et al., 1992) reported that the understanding of the thermal behavior of carbonate-apatite is complex.

TG-DTA experiment, conducted on the PN-8 sample under air, was compared to that conducted under the atmosphere (Fig. 6). It can be noticed that, in the first case (presence of oxygen), decarbonation reaction is slightly shifted to higher temperatures while departure of SO_3 is clearly shifted to higher temperatures.

Fig. 7a shows TG curves of three samples (PN-1, PN-2, PN-8) with variable quantities of calcite, as indicated by XRD (Fig. 7b). An examination of the curves trend in the 650–750 °C temperature interval, suggests that this is related

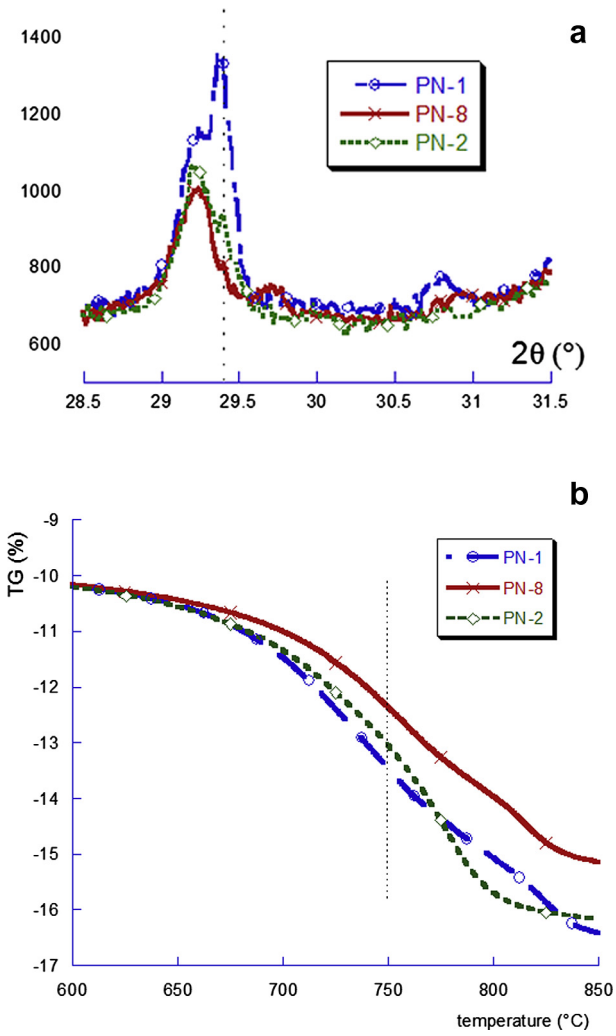

Figure 7 Evolution of carbonates content in phosphate samples as depicted by XRD (a) and TG (b) curves.

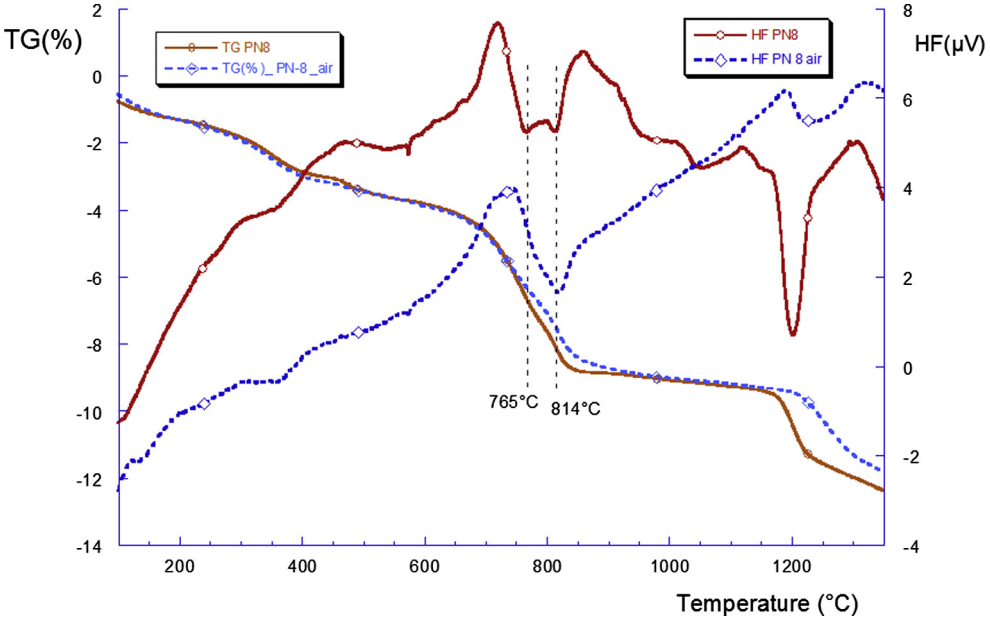

Figure 6 TG/DTA curves of the PN-8 sample obtained under air and He atmospheres.

to calcite decomposition, the second range (750–850 °C) is therefore associated to apatite decarbonation. This finding is confirmed by Lafon et al. (2003) who reported that the removal of CO_2 from apatite occurs in the 800–1050 °C temperature interval.

XRD quantification was carried out for the sample PN-8. The parameters that varied in refinements are: scale factor, lattice parameters, peak profile and preferred orientation for quartz. The background was fitted with simple interpolation. However, occupancies were not refined owing to the complicated phase mixture. The observed, calculated and residual profiles of patterns are reproduced in Fig. 8, which presents a good match between the measured and predicted diffractograms.

The quality of the Rietveld quantification was verified by the inspection of specific R values (R_{wp} = 11) as well as the check of the correlation matrix. Fig. 9 displays how one refined parameter is dependent or independent from other refined

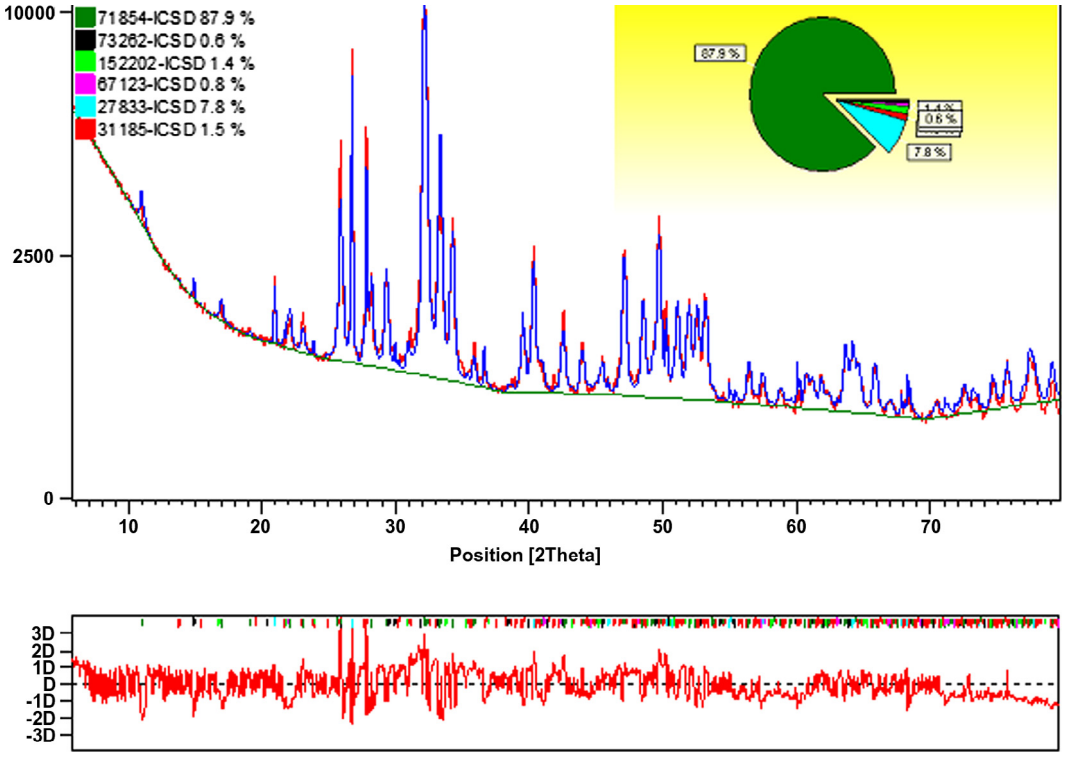

Figure 8 Observed, calculated and difference profiles for the Rietveld refinement for the phosphate sample PN-8.

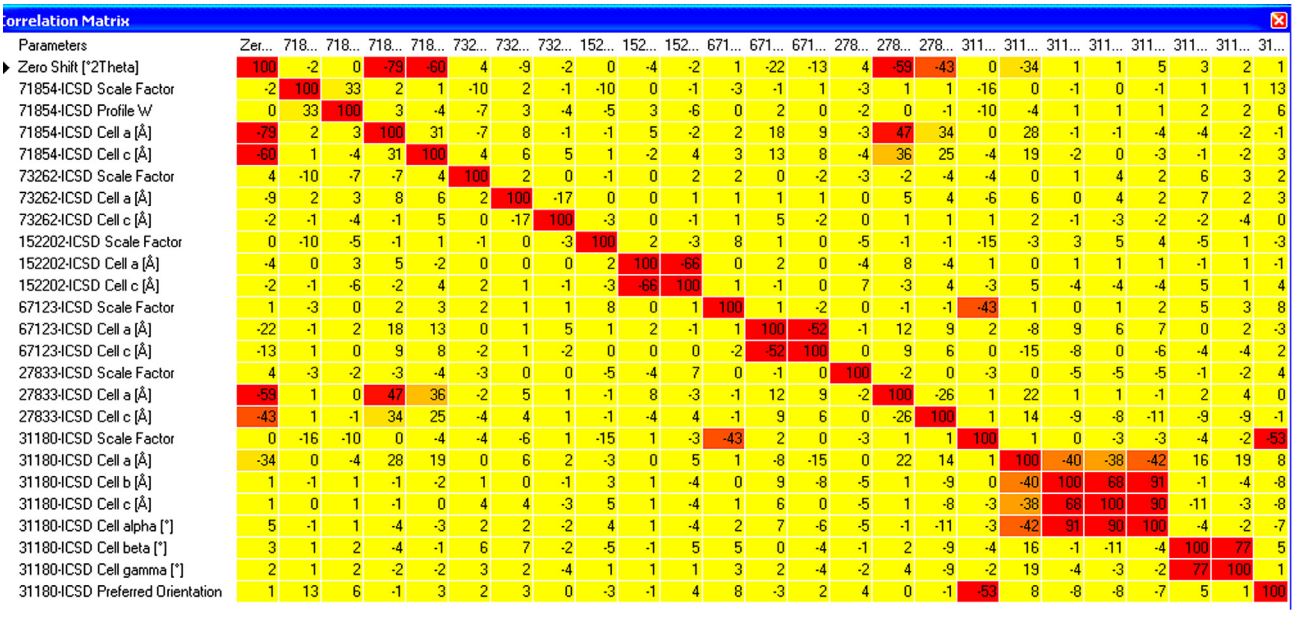

Figure 9 Correlation matrix of refinement parameters.

Table 2 Composition of sample PN8 as determined by the Rietveld refinement.

Mineral name	N° ICSD	Chemical formula	%
Apatite	71854	$Ca_{9.35}$ (P O4)$_{4.72}$ $F_{1.98}$ (C O_3)$_{1.483}$	87.9
Bassanite	73262	$CaSO_4$ 0.5 H_2O	0.6
Dolomite	152202	$CaMg(CO_3)_2$	1.4
Quartz	67123	SiO_2	0.8
Quartz	27833	SiO_2	7.8
Anorthoclase	31185	($Na_{0.85}$ $K_{0.15}$) (Al Si_3 O_8)	1.5

ones. A value of more or less 100, means a total dependency (positive or negative correlation), values of more or less than zero indicate no or very small dependencies, respectively. An inspection of this matrice reveals no dependence of phases scale factor with the rest of parameters. Therefore the observed correlation has no effect on the quantification result.

The quantitative analysis, using the Rietveld method, allowed to draw the composition given in Table 2, which displayed also the corresponding Inorganic Crystal-Structure Database (ICSD) code for the implicated phase used for quantification. For apatite, the structure model, whose calculated diffraction pattern best fits the experimentally-measured one, corresponds to the carbonate-apatite $Ca_{9.35}$ $(PO_4)_{4.72}$ $F_{1.98}$ $(CO_3)_{1.483}$ (ICSD n 71854) with refined cell parameters a = 9.329 A and c = 6.899 A. It should be emphasized that the apatite formula is schematic, since sodium and sulfate occur as minor constituents (Galfati et al., 2010).

The P_2O_5 and SiO_2 percentages, inferred from quantitative XRD data, are 28.2 and 9.6%, respectively, while equivalent proportions, determined by direct chemical analysis (AAS), amount to 26.75 and 8.66, respectively. The amount of CO_2 expected from the Rietveld data is 6.04% from apatite and 0.65% from dolomite while the TG analysis displayed a mass loss percentage between 575 and 900 °C equal to 5.13%.

The application of the Rietveld analysis to quantification of other samples (PN-1 to PN-7) has been limited due to misidentified phases, lack of model structure and relatively high amount of amorphous. Many of the secondary minerals, silicates in particular, are imperfectly crystallized, some having weak and broad XRD peaks and thus contribute to the non-diffracting part of the sample, yielding an underestimation of composition. Hence, the accuracy would be considerably improved if a structure model is made available for some minerals such as opal-CT.

All these findings show that XRD analysis can be a powerful tool conducive to systematic control analysis in industry. However, a number of reasons must be considered in terms of identification and refinement strategy: (i) some phases, for instance, calcite, gypsum and silicates crystallize with platy shapes showing preferred orientation effects; (ii) silica can crystallize as several polymorphs and (iii) ionic substitution.

4. Conclusion

In this study, phosphate ore samples' characterization of successive layers is carried out using the XRD, corroborated with many techniques (elementary analysis (AAS), thermal analysis TGA-DTA, carbon and sulfur analyzer, and FTIR). We have shown the Rietveld analysis can be a helpful adjunct to XRD in ascertaining the presence of minor mineral phases in natural phosphates. However the accuracy statement of such analysis and its degree of uncertainty are very important if this methodology is to be transferred to an industry as a routine tool for the process control. For this reason, an inter-laboratories program, based on quantitative phase analysis by powder diffraction, using the Rietveld method, would be necessary to evaluate its degree of uncertainty and accuracy and to assess its scope of validity and limitations. Further more work on combining elemental analysis (Chemscan or Mineral Liberation Analyzer), ssNMR, ATG-ATD and XRD is needed to improve the general structural formula of apatite.

Acknowledgement

The authors gratefully acknowledge the contribution of Mr. Wissem Majedi and Prof. Foued Suissi.

References

Abouzeid, A.Z.M., 2008. Physical and thermal treatment of phosphate ores – an overview. Int. J. Miner. Process. 85, 59–84.

Béji-Sassi, A., 1985. Pétrographie, minéralogie et géochimie des sédiments phosphatés de la bordure orientale de l'île de Kasserine (Tunisie). Thèse doct. Spécialité, Fac. Sc. Tunis,p. 230

Béji-Sassi, A., 1999. Les phosphates dans les bassins paléogènes de la partie méridionale de l'Axe Nord-Sud (Tunisie). Unpublished thesis Doctorat d'Etat ès-Sciences Géologiques, Université Tunis II, Tunisia, 424 pp.

Bigi, A., Falini, G., Foresti, E., Gazzono, M., Ripamonti, A., Roveri, N., 1996. Rietveld Structure refinements of calcium hydroxylapatite containing magnesium. Acta Crist. 52, 87–92.

Chaabani, F., 1995. Dynamique de la partie orientale du bassin de Gafsa au Crétacé et au Paléogène. Etude minéralogique et géochimique de la série phosphatée éocène. Tunisie méridionale. Unpublished thesis Doctorat d'Etat ès-Sciences Géologiques, Université Tunis II, Tunisie, 428 pp.

El-Jalead, I.S., Abouzeid, A.Z.M., El-Sinbawy, H.A., 1980. Calcination of phosphates: reactivity of calcined phosphate. Powder Technol. 26, 187–197.

Galfati, I., Béji Sassi, A., Zaïer, A., Bouchardon, J.L., Bilal, E., Joron, J.L., Sassi, S., 2010. Geochemistry and mineralogy of Paleocene-Eocene Oum El Khacheb phosphorites (Gafsa-Metlaoui Basin) Tunisia. Geochem. J. 44, 189–210.

Kampata, D., Naud, J., Sonnet, P., 2000. Adv. X-Ray Anal. 42, 379.

Lafon, J.P., Champion, E., Bernache-Assollant, D., Gibert, R., Danna, A.M., 2003. Thermal decomposition of carbonated calcium phosphate apatites. J. Therm. Anal. Cal. 73, 1127–1134.

León-Reina, L., De la Torre, A.G., Porrás-Vazquez, J.M., Cruz, M., Ordonez, L.M., Alcobé, X., Gispert-Guirado, F., Larrañaga-Varga, A., Paul, M., Fuellmann, T., Schmidt, R., Aranda, M.A.G., 2009. Round Robin on Rietveld quantitative phase analysis of Portland cements. J. Appl. Crystallogr. 42, 906–916.

Locardi, B.U., Gabbi, E.C., Profilo, B., 1993. Thermal behaviour of hydroxyl apatite intended for medical applications. Biomaterials 14, 437–441.

Mostafa, S.I., Bibawi, T.A., Yehia, A.A., Ibrahim, I.A., 2000. Dev. in Miner. Process. 13, C1-25–C1-31.

Notholt, A.J.G., Sheldon, R.P., Davidson, D.F., 1989. Phosphate deposits of the world. Phosphate Rock Resources, vol. 2. Cambridge University Press.

Omotoso, O., McCarty, D.K., Hiller, S., Kleeberg, R., 2006. Some successful approaches to quantitative mineral analysis as revealed by the 3rd Reynolds cup contest. Clays Clay Miner. 54, 748–760.

Pan, H., Darvell, B.W., 2010. Effect of carbonate on hydroxyapatite solubility. Cryst. Growth Des. 10, 845–850.

Petkova, V., Serafimova, Petrova, E.N., Pelovski, Y., 2011. Thermochemistry of triboactivated natural and NH4-exchanged clinoptilolite mixed with Tunisian apatite. J. Therm. Anal Calorim. 105, 535–544.

Rodriguez-Lorenzo, L.M., 2005. Studies on calcium deficient apatites structure by means of MAS-NMR spectroscopy. J. Mat. Sci. 16, 393–398.

Sassi, S., 1974. La sédimentation phosphatée au Paléocène dans le Sud et le Centre Ouest de la Tunisie. Unpublished thesis Doctorat d'Etat ès-Sciences, Orsay Paris France, 300.

Tõnsuaadu, K., Gross, K.A., Plūduma, L., 2012. A review on the thermal stability of calcium apatites. J. Therm. Anal. Calorim. 110, 647–659.

Veiderma, M., Tõnsuaadu, K., Knubovets, R., Peld, M., 2005. Impact of anionic substitutions on apatite structure and properties. J. Organomet. Chem. 690, 2638.

Vilbok, H., Knubovets, R., Veiderma, M., 1992. Synthesis and thermal transformations of Ca, Mg-carbonate apatite. Proc. Est. Acad. Sci. 41, 45–51.

Wilson, R.M., Elliott, J.C., Dowker, S.E., Smith, R., 2004. Rietveld structure refinement of precipitated carbonate apatite using neutron diffraction data. Biomaterials 25, 2205–2213.

Zaïer, A., 1999. Evolution tectno-sédimentaire du bassin phosphate du centre-Ouest de la Tunisie minéralogie, pétrographie, géochimie et genèse des phosphorites. Unpublished thesis Doctorat d'Etat ès-Sciences Géologiques, Université Tunis II, Tunisia, 370 pp.